Applied Physics A manuscript No.
(will be inserted by the editor)

Advances in gas-mediated electron beam induced etching and related material processing techniques

Milos Toth

Received: July 5, 2014/ Accepted: *Insert Date*

Abstract Electron beam induced etching (EBIE) has traditionally been used for top-down, direct-write, chemical dry etching and iterative editing of materials. The present article reviews recent advances in EBIE modeling and emerging applications, with an emphasis on use cases in which the approaches that have conventionally been used to realize EBIE are instead used for material analysis, surface functionalization, or bottom-up growth of nanostructured materials. Such applications are used to highlight the shortcomings of existing quantitative EBIE models, and to identify physico-chemical phenomena that must be accounted for in order to enable full exploitation and predictive modeling of EBIE and related electron beam fabrication techniques.

Keywords: electron beam induced etching, direct-write nanofabrication, nanostructures, surface functionalization, self-assembly, radiation effects, nanomaterials

PACS codes: 81.65.Cf, 81.07.-b, 79.60.Dp, 68.43.Mn, 68.43.-h, 82.30.Lp, 61.80.Fe, 61.80.-x, 81.16.Dn

1 Introduction

Gas-mediated electron beam induced etching (EBIE) is a direct-write, subtractive nanofabrication technique in which an electron beam and a precursor gas are used to realize chemical dry etching with a spatial resolution of $\sim$ 10 nm [1–5]. EBIE is typically performed using electron microscopes that are equipped with gas injectors, and enable *in-situ* imaging and analysis of the features fabricated by an electron beam. The technique is analogous to focused ion beam processing [6–11], but avoids damage, staining and redeposition artifacts caused by ion bombardment. EBIE is realized using gaseous precursors such as H_2O, O_2, NH_3, XeF_2, Cl_2 and SF_6, which have been used to volatilize a wide range of materials, including graphene [12], single [13] and multi-walled [14] C nanotubes, amorphous carbon [15–18], single crystal [19–22] and nano-crystalline [23] diamond, Si, SiO_2, Si_3N_4, Cr, Ti, TaN and photoresist [24–38]. Historical overviews and reviews of the EBIE technique and the underlying chemical pathways can be found in references [1–5]. The present article is focused on recent advances in EBIE modeling methods, and emerging applications of EBIE and related electron beam material restructuring, fabrication and analysis methods.

M. Toth*
School of Physics and Advanced Materials
University of Technology, Sydney
PO Box 123, Broadway, NSW 2007, Australia
E-mail: Milos.Toth@uts.edu.au

2 Mechanisms

EBIE precursor gases are injected into an electron microscope specimen chamber using one of two methods. Either a capillary is positioned near the electron beam impact point at the substrate surface, and used to inject the gas into a chamber that is pumped continuously using a high vacuum pumping system [39,40]. Alternatively, the entire vacuum chamber, or a sub-chamber [18] is filled with a precursor gas, as is done in environmental electron microscopy [41–44]. Ideally, the precursor gas does not etch the substrate spontaneously[1]. Instead, the chemical reactions that give rise to etching are driven by interactions between the inci-

[1] This is, however, not true in some cases, such as when XeF_2 is used for etching of Si [45,46,31], TaN [28], or TaBN

dent and emitted electrons, and surface-adsorbed precursor molecules (Fig. 1(a)). When an electron beam irradiates a substrate, precursor molecule adsorbates are consumed in the etch reaction, and the local surface concentration decreases to a steady state value, typically within ~ 1 millisecond [1]. The time-evolution of adsorbate concentration at each point on the surface is given by a competition between adsorbate consumption in etching, desorption, and adsorbate replenishment. The latter proceeds through adsorption from the gas phase and diffusion along the substrate surface (Fig. 1(b)). The vertical etch rate $(\partial z/\partial t)$ generally scales with the product of the electron flux, $f(x,y)$, and the concentration of surface-adsorbed precursor molecules, $N_a(x,y)$, at each point (x,y) on the substrate surface (Fig. 1(c)). It can be calculated as a function of electron beam irradiation time (t) by solving differential equations of the form [1,2]:

$$\frac{\partial N_a}{\partial t} = \Lambda - kN_a - \frac{\partial N_\alpha}{\partial t} + D\nabla^2 N_a, \tag{1}$$

$$\frac{\partial z}{\partial t} = V\frac{\partial N_\alpha}{\partial t} = V\sigma f N_a, \tag{2}$$

where a and α signify surface-adsorbed precursor molecules and dissociation products, respectively; Λ, kN_a and $\frac{\partial N_\alpha}{\partial t}$ are the adsorption, desorption and electron induced dissociation rates (per unit area), and D is the precursor adsorbate diffusion coefficient. The constant V is the volume of a single molecule removed from the substrate in the etch reaction, and σ is an electron scattering cross-section for the activated process that leads to volatilization[2]. Adsorption is usually assumed to proceed through a single physisorbed state (Fig. 2(a)), and surface coverage is normally limited to 1 ML by the Langmuir isotherm:

$$\Lambda = sF(1-\Theta), \tag{3}$$

where s is the sticking coefficient, $F(x,y)$ is the gas molecule flux at the substrate surface (given by the gas pressure and temperature), and $\Theta(x,y,)$ is the precursor adsorbate coverage.

The above modeling approach is also applicable to the related technique of electron beam induced deposition (EBID) [1–5,47–49], and is often used in studies of deposition and etch kinetics. Reaction rate kinetics are of interest because they affect spatial resolution, proximity effects, fabrication rates, composition and the topography of nanostructures fabricated by EBIE and EBID [50–53,49,54,23,55,16]. In recent years, the basic model defined by Eqns. 1–2 has been used (or modified) to account for the following phenomena:

- *The gas pressure distribution inside the electron microscope specimen chamber* [39,40,56,57], which governs the gas molecule flux $F(x,y)$ across the substrate surface. The precursor pressure can vary substantially across the surface region irradiated by the electron beam, particularly when the precursor gas is delivered into the vacuum chamber using a capillary located near the beam impact point at the surface. Pressure distributions are significant because they causes the EBIE rate to vary across the substrate surface through Eqn. 3.
- *Precursor transport into high aspect ratio pits* [55]. The gas flow conductance of a pit decreases with increasing aspect ratio, and hence alters the replenishment rate of precursor molecules consumed in EBIE. The replenishment rate affects N_a which determines the etch rate through Eqn. 2. Etch pit conductance can be the dominant, etch-rate-limiting process when fabricating high aspect ratio pits. It causes the etch rate to decrease as the etch pit grows during EBIE, giving rise to a characteristic, sublinear dependence of etch pit depth on electron beam processing time [55].
- *The behavior of etch reaction products* (α) *at the substrate surface* [58]. The diffusion, desorption, and electron induced re-dissociation of etch product molecules can be modeled by setting up a differential equation analogous to Eqn. 1 for each molecular species at the substrate surface. Etch reaction product kinetics are relevant if the molecules have a significant residence time at the surface, or if multiple reaction steps are needed to produce a volatile species that ultimately desorbs from the surface. Electron induced dissociation of reaction products acts to reverse EBIE. It can limit the etch rate, and can give rise to complex dependencies of etch rate on electron flux [58].
- *EBIE performed using a precursor gas mixture* comprised of an etch precursor and a deposition precursor [16,54]. Mixtures are implemented by setting up a differential equation for each molecular species making up the gas, and can be used to simulate the resulting dependencies of the etch (and deposition) rate on electron flux. Mixtures play a role in EBIE

[27], where delocalized etching occurs spontaneously and the electron beam is used to accelerate the local etch rate.

[2] It is usually assumed that electrons dissociate precursor molecule adsorbates, thereby generating reactive fragments which react with and volatilize the substrate [1]. Hence, σ is an 'effective' [23] cross-section for fragment generation. However, in some cases, such as XeF_2 EBIE of SiO_2 [26] and XeF_2 EBIE of Si_3N_4 [30], etching has been argued to proceed through a cyclic process of electron induced removal of O (or N) from the substrate surface, and spontaneous etching of excess Si by XeF_2. Such processes can be modeled by the above equations provided that σ is taken to represent a cross-section for the electron induced restructuring step that leads to the removal of O (or N) from the surface.

when residual contaminants such as hydrocarbons are present in the vacuum chamber and give rise to unintended EBID that competes with etching [18, 29, 16]. Mixtures can also be used to intentionally modify and control reaction kinetics, and hence control the morphology [54] or composition [59–61, 53, 62–66, 49, 67] of nanostructures fabricated by electron beam fabrication techniques.

- *The potential well and energy barrier associated with activated chemisorption* [68], a type of adsorption in which a gas molecule overcomes an energy barrier and forms a chemical bond with a surface (Fig. 2(b)). Activated chemisorption alters the temperature dependence of the adsorbate concentration N_a, and enables electron beam chemical processing at elevated temperatures where the surface coverage of physisorbed precursor molecules is negligible. This has a number of benefits such as accelerated desorption of unwanted adsorbates (e.g. C-containing contaminants), and enables control over the species of surface-adsorbed precursor molecules through partial, thermal decomposition of the adsorbates.
- *Spontaneous decomposition of precursor molecules at the substrate surface*, which can occur in parallel with electron induced dissociation. This effect has been modeled for the case of XeF_2 [69] which can fragment through a dissociative chemisorption pathway, leading to fluorination of many surfaces [45, 46, 70, 71] at room temperature. The model used to simulate the spontaneous and electron induced dissociation of XeF_2 [69] is a variant of a model of activated chemisorption [68] that had been developed to describe the temperature-dependence of EBID preformed using tetraethoxysilane (TEOS) as the precursor gas.
- *Chemically active (and inactive) surface sites that enable (or inhibit) EBIE*, and dynamic activation of surface sites through electron beam restructuring of the substrate [23]. Surface site activation can enable EBIE of materials that can not be etched in their virgin, unmodified state. It can also alter etch kinetics, and give rise to a characteristic super-linear dependence of etch pit depth on electron beam processing time.

The above continuum models of EBIE [16, 23, 54, 55, 58, 69] and analogous (continuum and Monte Carlo) models of EBID have been used to simulate the time-evolution of the geometries (and in some cases the composition [53]) of structures fabricated by these techniques. The key limitations of existing models are that: (i) the model input parameters are often not known for precursor-substrate combinations of interest, (ii) changes in sample geometry caused by EBIE (or EBID) and their consequences for the electron flux profile, $f(x, y)$, have not been modeled realistically over large areas and for long processing times, and (iii) all of the individual effects listed above have thus far been studied in isolation, and are yet to be consolidated into a generic, predictive model of etching and deposition. Furthermore, a number of physical and chemical processes have, to date, not been incorporated explicitly in published EBIE models. These include electron stimulated desorption [72–74], knock-on damage and sputtering caused by high energy ($\gtrsim$ 100 keV) electrons and other mechanisms through which an electron beam can alter the substrate composition and nanostructure [75–82], the use of actual (rather than effective [23]) cross-sections for EBIE, realistic multi-step reaction pathways, surface roughening caused by EBIE (Fig. 3(a-d)), electron beam induced heating [83], and the effects of charging [84] caused by electron injection into insulators or electrically isolated substrate regions.

3 Applications

Traditionally, EBIE has been used as a direct-write subtractive nanofabrication technique (Fig. 3(a-h)). Sample applications include iterative editing of individual nanostructures [85, 19], repair of photolithographic masks [27, 28], fabrication of nanopores in membranes [30, 35], etching of 3D in-plane features in photoresist [37], and re-shaping of tips used in scanning probe microscopy [33, 38]. EBIE has also been used to improve the purity of materials grown by EBID. This application exploits the fact that EBIE is a material-specific chemical etch process. A gas mixture comprised of a deposition precursor (e.g. $Au(CH_3)_2(C_5H_7O_2)$) and an etch precursor (e.g. H_2O) is used to deposit a material such as Au and simultaneously etch impurities (C) that are unintentionally co-deposited during EBID. The gas mixing method has been used to purify EBID-grown Au [62–65], Pt [66], Fe_3O_4 [61] and SiO_2 nanostructures [59, 60, 86].

Vanhove *et al.* [87, 31, 88] have developed a material characterization technique in which gaseous EBIE reaction products are ionized by ultra-short laser pulses (above the substrate surface) and analyzed by a mass spectrometer. This innovative method enables depth-resolved analysis of solids, and fundamental studies of EBIE mechanisms that lead to volatilization.

Recently, precursors that are conventionally used for EBIE have been used to achieve other forms of material restructuring. This has been demonstrated most dramatically using XeF_2, which can be used to realize three distinct processes (Fig. 4(a-c)): electron beam induced fluorination of surfaces [69, 89], conventional EBIE, and

growth of GaF_3-containing microstructures [90]. Fluorination (Fig. 4(a)) has bee used to functionalize a range of surfaces, and to develop a deposition process in which F-terminated surface regions are used to catalyze chemical reactions that initiate localized, room temperature chemical vapor deposition [69]. The key, distinguishing aspect of this electron beam writing technique (Fig. 4(a)) is that the function of the beam is to remove surface-terminating molecules and replace them with a chemisorbed species such as fluorine (as opposed to the removal of bulk material from the substrate, as is done in conventional EBIE, Fig. 4(b)). The technique is a variant of similar methods used to fabricate chemically active surface regions [91–97], and electron irradiation methods used in surface chemistry studies of phenomena such as electron induced oxidation [98].

Electron induced dissociation of XeF_2 adsorbates can also be used to fabricate GaF_3-containing microstructures (Fig. 4(c)) through a spontaneous, chemically-assisted structure formation mechanism driven by a charged particle beam [90]. Specifically, a focused Ga^+ ion beam is used to induce bottom-up growth of Ga-filled, GaF_3 microcapillaries by irradiating a GaN substrate in the presence of XeF_2 precursor gas. The GaF_3 structures form as a result of electron induced decomposition of XeF_2 adsorbates on a surface that contains excess Ga. The electrons that dissociate XeF_2 are secondary electrons emitted from GaN as a result of ion irradiation.

Finally, Lassiter *et al.* [99] have used electron beam irradiation in a H_2O environment to iteratively edit the geometry and modify the plasmonic properties of a single (gold shell – silica core) nanoparticle. In this work, chemical etching was excluded as the underlying mechanism which was ascribed to a form of ablation assisted by heating and charging. This application illustrates the potential of direct-write, electron beam writing techniques for iterative editing of active, functional nanostructures.

3.1 The gap between applications and present modeling capability

The above applications highlight the need for advances in predictive, quantitative modeling of electron (and ion) beam induced etching, deposition and restructuring of solids in gaseous environments. For example, EBIE models are needed to improve present understanding of surface roughening that occurs during etching, and typically limits the spatial resolution and geometries of sub-10 nm features fabricated by EBIE [85] (see Fig. 3(a-d)). Roughening must be minimized to improve EBIE resolution and the depth resolution of the EBIE-based mass-spectroscopic analysis technique developed by Vanhove *et al.* [88].

Furthermore, existing models can not simulate: (i) heat- and charge-assisted restructuring processes such as that proposed by Lassiter *et al.* [99], (ii) the growth and size distribution of nanocrystallites grown by EBID (which are known to depend on fabrication conditions [79–82, 67]), and (iii) the clustering and spatial distribution of impurities present in deposits that were grown by conventional EBID or purified by gas mixtures that give rise to simultaneous EBID and EBIE [59–66, 86]. Predictive models of these phenomena will improve our ability to tune material functionality by controlling composition, internal nanostructure and feature geometry at the sub-10 nm scale.

Electron beam induced fluorination (Fig. 4(a)) has been modeled in detail, but the process of spontaneous deposition catalyzed by chemisorbed fluorine has not been modeled [69]. Similarly, the spontaneous growth of the Ga-filled microstructures shown in Fig. 3(i) and 4(c) was simulated by a mass transport model that helped explain the self-organized structure formation mechanism [90]. However, this new form of bottom-up growth has not been incorporated into standard models of particle beam processing (such as Eqns. 1-3). A unified model would improve present understanding of the scope and applicability of chemically-assisted electron and ion beam processing methods in terms of throughput, resolution, feature placement accuracy, and the geometries, composition and complexity of materials that can be fabricated by these techniques.

4 Outlook

Recent applications of electron beam writing techniques have blurred the distinction between EBIE and related deposition methods by demonstrating that precursors which have conventionally been used for etching can also be used to functionalize surfaces [69, 89] and to grow complex, non-planar microstructures [90]. These developments, and other examples of surface activation [91–97] and nanostructure editing through non-chemical pathways [99], highlight the wide diversity of processes that can be exploited by electron beam processing techniques. Furthermore, these recent applications illustrate the need for advances in predictive modeling of electron (and ion) beam restructuring of materials in both inert and reactive environments. Models published to date have been used to explain a range of isolated etching, deposition and surface restructuring phenomena. However, the models neglect numerous physical and chemical mechanisms and can not describe effects such as surface roughening and the simultaneous evolution of surface topology, internal nanos-

tructure and composition of materials fabricated or restructured by charged particle beams. Future work will likely address these shortcomings, and lead to a better understanding of the full potential of EBIE and related material restructuring [69, 90–97] and characterization [87, 31, 88] techniques.

References

1. I. Utke, S. Moshkalev, P. Russell, *Nanofabrication Using Focused Ion and Electron Beams. Principles and Applications* (Oxford University Press, USA, 2012)
2. I. Utke, A. Goelzhaeuser, Angew Chem Int Edit **49**(49), 9328 (2010)
3. C.R. Arumainayagam, H.L. Lee, R.B. Nelson, D.R. Haines, R.P. Gunawardane, Surf. Sci. Rep. **65**(1), 1 (2010)
4. I. Utke, P. Hoffmann, J. Melngailis, J. Vac. Sci. Technol. B **26**(4), 1197 (2008)
5. S.J. Randolph, J.D. Fowlkes, P.D. Rack, Cr Rev Solid State **31**(3), 55 (2006)
6. C.S. Kim, S.H. Ahn, D.Y. Jang, Vaccum **86**(8), 1014 (2012)
7. R. Kometani, S. Ishihara, Sci. Technol. Adv. Mater. **10**(3), 034501 (2009)
8. S. Matsui, Y. Ochiai, Nanotechnology **7**, 274 (1996)
9. A.A. Tseng, J. Micromech. Microeng. **14**(4), R15 (2004)
10. A.A. Tseng, Small **1**(10), 924 (2005)
11. F. Watt, A.A. Bettiol, J.A. Van Kan, E.J. Teo, M. Breese, International Journal of Nanoscience **4**(03), 269 (2005)
12. S. Goler, V. Piazza, S. Roddaro, V. Pellegrini, F. Beltram, P. Pingue, J. Appl. Phys. **110**(6), 064308 (2011)
13. C. Thiele, M. Engel, F. Hennrich, M.M. Kappes, K.P. Johnsen, C.G. Frase, H.V. Loehneysen, R. Krupke, Appl. Phys. Lett. **99**(17), 173105 (2011)
14. P.S. Spinney, D.G. Howitt, S.D. Collins, R.L. Smith, Nanotechnology **20**(46), (2009)
15. D. Wang, Hoyle, P. C., J.R.A. Cleaver, G.A. Porkolab, N.C. Macdonald, J. Vac. Sci. Technol. B **13**(5), 1984 (1995)
16. M. Toth, C.J. Lobo, G. Hartigan, W.R. Knowles, J. Appl. Phys. **101**(5), 054309 (2007)
17. H. Miyazoe, I. Utke, J. Michler, K. Terashima, Appl. Phys. Lett. **92**(4), 043124 (2008)
18. C.J. Lobo, A. Martin, M.R. Phillips, M. Toth, Nanotechnology **23**(37), 375302 (2012)
19. A.A. Martin, M. Toth, I. Aharonovich, Sci. Rep. **4**, 5022 (2014)
20. P. Hoffmann, I. Utke, A. Perentes, T. Bret, C. Santschi, V. Apostolopoulos, Proc. SPIE **5925**, 592506 (2005)
21. J. Niitsuma, X. Yuan, S. Koizumi, T. Sekiguchi, Jpn. J. Appl. Phys., Part 2 **45**(1–3), L71 (2006)
22. J. Taniguchi, I. Miyamoto, N. Ohno, K. Kantani, M. Komuro, H. Hiroshima, Jpn. J. Appl. Phys. **36**, 7691 (1997)
23. A.A. Martin, M.R. Phillips, M. Toth, ACS Appl. Mater. Interfaces **5**(16), 8002 (2013)
24. P.D. Rack, S. Randolph, Y. Deng, J. Fowlkes, Y. Choi, D.C. Joy, Appl. Phys. Lett. **82**(14), 2326 (2003)
25. J.H. Wang, D.P. Griffis, R. Garcia, P.E. Russell, Semicond. Sci. Technol. **18**(4), 199 (2003)
26. S.J. Randolph, J.D. Fowlkes, P.D. Rack, J. Appl. Phys. **98**(3), 034902 (2005)
27. T. Liang, E. Frendberg, B. Lieberman, A. Stivers, J. Vac. Sci. Technol. B **23**(6), 3101 (2005)
28. M.G. Lassiter, T. Liang, P.D. Rack, Journal of Vacuum Science and Technology B: Microelectronics and Nanometer Structures **26**(3), 963 (2008)
29. M. Toth, C.J. Lobo, M.J. Lysaght, A.E. Vladar, M.T. Postek, J. Appl. Phys. **106**(3), 034306 (2009)
30. M. Yemini, B. Hadad, Y. Liebes, A. Goldner, N. Ashkenasy, Nanotechnology **20**(24), 245302 (2009)
31. N. Vanhove, P. Lievens, W. Vandervorst, Phys. Rev. B **79**(3), 035305 (2009)
32. N. Vanhove, P. Lievens, W. Vandervorst, J. Vac. Sci. Technol. B **28**(6), 1206 (2010)
33. J.H. Noh, M. Nikiforov, S.V. Kalinin, A.A. Vertegel, P.D. Rack, Nanotechnology **21**(36) (2010)
34. F.J. Schoenaker, R. Córdoba, R. Fernández-Pacheco, C. Magén, O. Stéphan, C. Zuriaga-Monroy, M.R. Ibarra, J.M. De Teresa, Nanotechnology **22**(26), 265304 (2011)
35. Y. Liebes, B. Hadad, N. Ashkenasy, Nanotechnology **22**(28), 285303 (2011)
36. P. Roediger, H.D. Wanzenboeck, S. Waid, G. Hochleitner, E. Bertagnolli, Nanotechnology **22**(23), (2011)
37. J.M. Perry, Z.D. Harms, S.C. Jacobson, Small **8**(10), 1521 (2012)
38. N.A. Roberts, J.H. Noh, M.G. Lassiter, S. Guo, S.V. Kalinin, P.D. Rack, Nanotechnology **23**(14), 145301 (2012)
39. V. Friedli, I. Utke, J. Phys. D **42**(12), 125305 (2009)
40. I. Utke, V. Friedli, S. Amorosi, J. Michler, P. Hoffmann, Microelectronic Engineering **83**(4-9), 1499 (2006)
41. D.F. Parsons, Science **186**, 407 (1974)
42. G.D. Danilatos, Adv. Electron. El. Phys. **71**, 109 (1988)
43. M. Toth, W.R. Knowles, B.L. Thiel, Appl. Phys. Lett. **88**(2), 023105 (2006)
44. M. Toth, M. Uncovsky, W.R. Knowles, F.S. Baker, Appl. Phys. Lett. **91**(5), 053122 (2007)
45. H.F. Winters, J.W. Coburn, Appl. Phys. Lett. **34**(1), 70 (1979)
46. Y.Y. Tu, T.J. Chuang, H.F. Winters, Phys. Rev. B **23**(2), 823 (1981)
47. W.F. van Dorp, C.W. Hagen, J. Appl. Phys. **104**, 081301 (2008)
48. A. Botman, J.J.L. Mulders, C.W. Hagen, Nanotechnology **20**(37), 372001 (2009)
49. M. Huth, F. Porrati, C. Schwalb, M. Winhold, R. Sachser, M. Dukic, J. Adams, G. Fantner, Beilstein J. Nanotechnol. **3**, 597 (2012)
50. J.D. Fowlkes, P.D. Rack, ACS Nano **4**(3), 1619 (2010)
51. D.A. Smith, J.D. Fowlkes, P.D. Rack, Nanotechnology **18**(26) (2007)
52. D.A. Smith, J.D. Fowlkes, P.D. Rack, Small **4**(9), 1382 (2008)
53. L. Bernau, M. Gabureac, R. Erni, I. Utke, Angew Chem Int Edit **49**(47), 8880 (2010)
54. C.J. Lobo, M. Toth, R. Wagner, B.L. Thiel, M. Lysaght, Nanotechnology **19**(2), 025303 (2008)
55. S. Randolph, M. Toth, J. Cullen, C. Chandler, C. Lobo, Appl. Phys. Lett. **99**(21), 213103 (2011)
56. G.D. Danilatos, M.R. Phillips, J.V. Nailon, Micros. Microanal. **7**(5), 397 (2001)
57. G. Danilatos, J. Microsc.-Oxford **234**, 26 (2009)
58. M.G. Lassiter, P.D. Rack, Nanotechnology **19**(45), 455306 (2008)
59. A. Perentes, P. Hoffmann, J. Vac. Sci. Technol. B **25**(6), 2233 (2007)
60. A. Perentes, P. Hoffmann, Chem. Vapor Depos. **13**(4), 176 (2007)
61. M. Shimojo, M. Takeguchi, K. Furuya, Nanotechnology **17**(15), 3637 (2006)

62. A. Folch, J. Tejada, C.H. Peters, M.S. Wrighton, Appl. Phys. Lett. **66**(16), 2080 (1995)
63. A. Folch, J. Servat, J. Esteve, J. Tejada, M. Seco, J. Vac. Sci. Technol. B **14**(4), 2609 (1996)
64. K. Molhave, D.N. Madsen, A.M. Rasmussen, A. Carlsson, C.C. Appel, M. Brorson, C.J.H. Jacobsen, P. Boggild, Nano Lett. **3**(11), 1499 (2003)
65. K. Molhave, D.N. Madsen, S. Dohn, P. Boggild, Nanotechnology **15**(8), 1047 (2004)
66. S. Wang, Y.M. Sun, Q. Wang, J.M. White, J. Vac. Sci. Technol. B **22**(4), 1803 (2004)
67. F. Porrati, B. Kämpken, A. Terfort, M. Huth, J. Appl. Phys. **113**(5), 053707 (2013)
68. J. Bishop, C.J. Lobo, A. Martin, M. Ford, M.R. Phillips, M. Toth, Phys. Rev. Lett. **109**, 146103 (2012)
69. S.J. Randolph, A. Botman, M. Toth, Particle **30**(8), 672 (2013)
70. M. Loudiana, A. Schmid, J. Dickinson, E. Ashley, Surf. Sci. **141**, 409 (1984)
71. M. Hills, G. Arnold, Appl. Surf. Sci. **47**(1), 77 (1991)
72. R.D. Ramsier, J.T. Yates, Surf. Sci. Rep. **12**(6-8), 243 (1991)
73. W. Li, D.C. Joy, J. Vac. Sci. Technol. A **24**(3), 431 (2006)
74. W.F. van Dorp, T.W. Hansen, J.B. Wagner, J.T.M. De Hosson, Beilstein J. Nanotechnol. **4**, 474 (2013)
75. F. Banhart, Rep. Prog. Phys. **62**(8), 1181 (1999)
76. R.F. Egerton, P. Li, M. Malac, Micron **35**(6), 399 (2004)
77. R.F. Egerton, R. McLeod, F. Wang, M. Malac, Ultramicroscopy **110**(8), 991 (2010)
78. A.V. Krasheninnikov, K. Nordlund, J. Appl. Phys. **107**(7), 071301 (2010)
79. A. Botman, C.W. Hagen, J. Li, B.L. Thiel, K.A. Dunn, J.J.L. Mulders, S. Randolph, M. Toth, J. Vac. Sci. Technol. B **27**(6), 2759 (2009)
80. J. Li, M. Toth, V. Tileli, K.A. Dunn, C.J. Lobo, B.L. Thiel, Appl. Phys. Lett. **93**(2), 023130 (2008)
81. J.T. Li, M. Toth, K.A. Dunn, B.L. Thiel, J. Appl. Phys. **107**(10), 103540 (2010)
82. F. Porrati, R. Sachser, C.H. Schwalb, A.S. Frangakis, M. Huth, J. Appl. Phys. **109**(6) (2011)
83. S.J. Randolph, J.D. Fowlkes, P.D. Rack, J. Appl. Phys. **97**(12), 124312 (2005)
84. J. Cazaux, J. Appl. Phys. **95**(2), 731 (2004)
85. M. Toth, C.J. Lobo, W.R. Knowles, M.R. Phillips, M.T. Postek, A.E. Vladar, Nano Lett. **7**(2), 525 (2007)
86. J. Bishop, M. Toth, M. Phillips, C. Lobo, Appl. Phys. Lett. **101**(21), 211605 (2012)
87. N. Vanhove, P. Lievens, W. Vandervorst, Appl. Surf. Sci. **255**(4), 1360 (2008)
88. N. Vanhove, P. Lievens, W. Vandervorst, Surf. Interface Anal. **43**(1-2), 159 (2010)
89. T. Shanley, A.A. Martin, I. Aharonovich, M. Toth, Appl. Phys. Lett. **in press** (2014)
90. A. Botman, A. Bahm, S. Randolph, M. Straw, M. Toth, Phys. Rev. Lett. **111**(13), 135503 (2013)
91. T. Lukasczyk, M. Schirmer, H.P. Steinruck, H. Marbach, Langmuir **25**(19), 11930 (2009)
92. M. Walz, M. Schirmer, F. Vollnhals, T. Lukasczyk, H.P. Steinruck, H. Marbach, Angewandte Chemie-international Edition **49**, 4669 (2010)
93. F. Vollnhals, P. Wintrich, M.M. Walz, H.P. Steinruck, H. Marbach, Langmuir **29**(39), 12290 (2013)
94. F. Vollnhals, T. Woolcot, M.M. Walz, S. Seiler, H.P. Steinruck, G. Thornton, H. Marbach, The Journal of Physical Chemistry C **117**(34), 17674 (2013)
95. M.M. Walz, F. Vollnhals, F. Rietzler, M. Schirmer, H.P. Steinruck, H. Marbach, Appl. Phys. Lett. **100**(5), 053118 (2012)
96. K. Muthukumar, H.O. Jeschke, R. Valentí, E. Begun, J. Schwenk, F. Porrati, M. Huth, Beilstein J. Nanotechnol. **3**, 546 (2012)
97. M.N. Khan, V. Tjong, A. Chilkoti, M. Zharnikov, Angew Chem Int Edit **51**(41), 10303 (2012)
98. H. Ebinger, J. Yates, Phys. Rev. B **57**(3), 1976 (1998)
99. J.B. Lassiter, M.W. Knight, N.A. Mirin, N.J. Halas, Nano Lett. **9**(12), 4326 (2009)

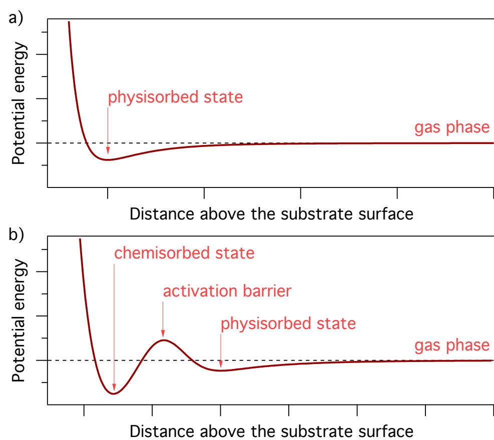

Fig. 2 Potential energy diagrams for physisorption (a) and activated chemisorption (b) used in models of gas-mediated electron beam induced processing [68,69].

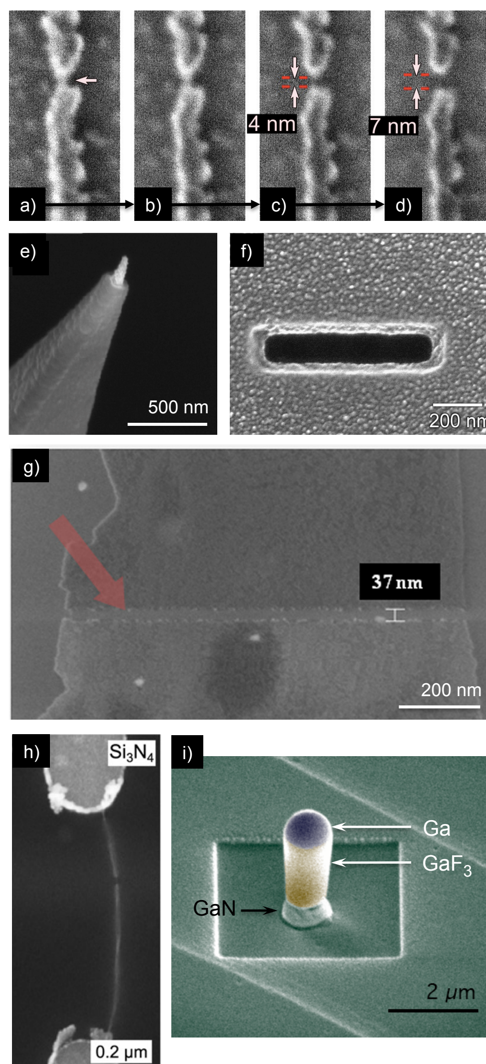

Fig. 3 (a-d) Four frames from a movie showing the formation of a nano-gap in a carbonaceous nanowire on a bulk SiO_2 substrate by high resolution, H_2O EBIE [85], (e) scanning probe microscopy tip sculpted by XeF_2 EBIE [38], (f) etch pit in chrome fabricated by XeF_2 EBIE [16], (g) 37 nm gap etched in graphene by O_2 EBIE [12], (h) gap cut into a single-walled carbon nanotube by O_2 EBIE [13], (i) false-color electron image of a Ga-filled GaF_3 microcapillary grown using XeF_2 as shown in Fig. 4(c) [90].

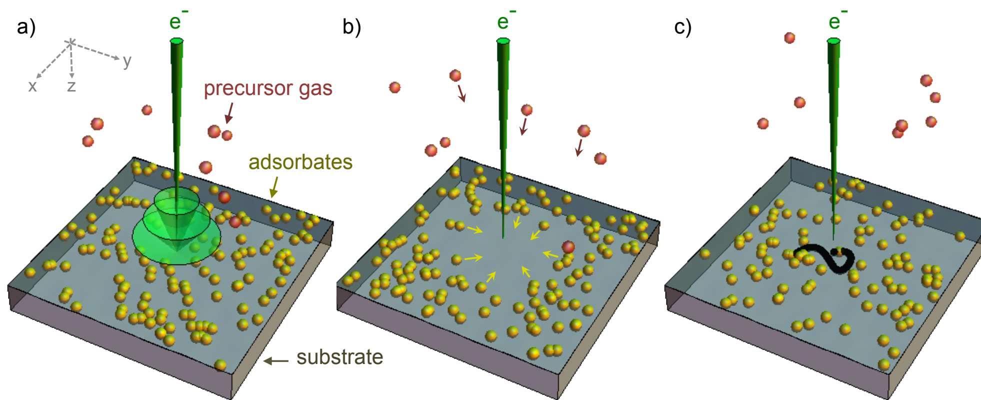

Fig. 1 General steps involved in electron beam induced etching: (a) electron beam irradiation, and emission of secondary and backscattered electrons from the substrate, (b) consumption of adsorbates in the etch reaction, and precursor replenishment through adsorption from the gas phase and diffusion along the substrate surface, (c) volatilization of the substrate in the vicinity of the electron beam.

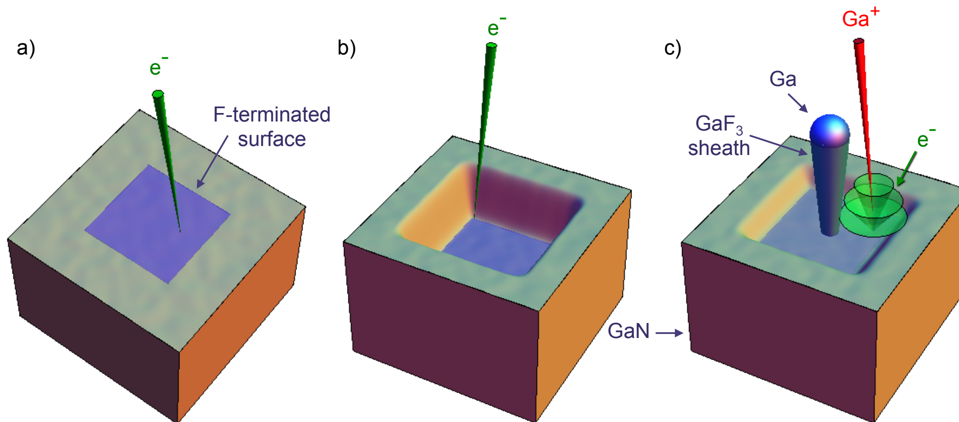

Fig. 4 Three forms of material processing driven by electron dissociation of XeF_2 adsorbates: (a) fluorination of the substrate surface [69], (b) electron beam induced etching, and (c) fabrication of gallium-filled, GaF_3 capillaries by ion bombardment of GaN [90]. GaF_3 forms due to XeF_2 decomposition by secondary electrons which are emitted from GaN and irradiate the sidewall of the growing pillar. An electron image of such a microstructure is shown in Fig. 3(i)